NIH Public Access
Author Manuscript
Lab Chip. Author manuscript; available in PMC 2014 March 21.

Published in final edited form as:
Lab Chip. 2013 March 21; 13(6): 1093–1101. doi:10.1039/c2lc41208j.

SyM-BBB: A Microfluidic Blood Brain Barrier Model

Balabhaskar Prabhakarpandian[1], **Ming-Che Shen**[1], **Joseph B. Nichols**[1], **Ivy R. Mills**[1], **Marta Sidoryk-Wegrzynowicz**[2], **Michael Aschner**[2,3,4], and **Kapil Pant**[1]

[1]Biomedical Technology, CFD Research Corporation, Huntsville, AL 35805

[2]Department of Pediatrics, Vanderbilt University Medical Center, Nashville, TN 37232

[3]Kennedy Center for Research on Human Development, Vanderbilt University Medical Center, Nashville, TN 37232

[4]Department of Pharmacology, Vanderbilt University Medical Center, Nashville, TN 37232

Abstract

Current techniques for mimicking the Blood-Brain Barrier (BBB) largely use incubation chambers (Transwell) separated with a filter and matrix coating to represent and to study barrier permeability. These devices have several critical shortcomings; (a) they do not reproduce critical microenvironmental parameters, primarily anatomical size or hemodynamic shear stress, (b) they often do not provide real-time visualization capability, and (c) they require a large amount of consumables. To overcome these limitations, we have developed a microfluidics based Synthetic Microvasculature model of the Blood-Brain Barrier (SyM-BBB). The SyM-BBB platform is comprised of a plastic, disposable and optically clear microfluidic chip with a microcirculation sized two-compartment chamber. The chamber is designed in such a way as to permit the realization of side-by-side apical and basolateral compartments, thereby simplifying fabrication and facilitating integration with standard instrumentation. The individually addressable apical side is seeded with endothelial cells and the basolateral side can support neuronal cells or conditioned media. In the present study, an immortalized Rat Brain Endothelial cell line (RBE4) was cultured in SyM-BBB with a perfusate of Astrocyte Conditioned Media (ACM). Biochemical analysis showed upregulation of tight junction molecules while permeation studies showed an intact BBB. Finally, transporter assay was successfully demonstrated in SyM-BBB indicating a functional model.

Introduction

Delivery of neuroprotective or therapeutic agents to specific regions of the brain presents a major challenge, largely due to the presence of the Blood-Brain Barrier (BBB). Physiologically, the BBB consists of an intricate network of vascular endothelial cells (ECs) that isolate the central nervous system (CNS) from systemic blood circulation except the circumventricular organs. A combination of physical and biochemical barriers establishes the BBB endothelium as quite distinct from other endothelia[1-5]. The BBB is formed by capillary endothelial cells, surrounded by basal lamina and astrocytic perivascular endfeet with astrocytes providing the cellular link to the neurons. The astrocyte endfeet form an envelope around the blood vessels and are attached to the basement membrane tightly by their adhesion molecules. The basement membrane is composed of extracellular matrix molecules such as type IV collagen, laminins, fibronectin, heparan sulfates, and proteoglycans. An intact basement membrane provides structural support to the cells and is also critical in delivering communicative signals between the intravascular components and the glial/neuronal cells in addition to nutritional support from the blood stream[6]. The microcapillary endothelium is characterized by the presence of tight junctions, a lack of fenestrations and minimal pinocytotic vesicles[7]. Small (<500 Da) lipid-soluble substances

NIH-PA Author Manuscript
NIH-PA Author Manuscript
NIH-PA Author Manuscript

NIH-PA Author Manuscript

NIH-PA Author Manuscript

NIH-PA Author Manuscript

such as alcohol, narcotics and anticonvulsants, are believed to pass through the BBB with relative ease. However for most other substances, tight junctions between the cerebral ECs form a diffusion barrier. Even in the event of successful crossing of the barrier, the drug efflux pump P-glycoprotein (Pgp), an important component of the BBB, pumps recognized substrates from the CNS thereby limiting exposure. The tight junction consists of transmembrane proteins (claudin, occludin, and junction adhesion molecules) and cytoplasmic accessory proteins. Claudins form dimers and bind to claudins on adjacent endothelial cells to establish the primary gate of the tight junction. The main functions of occludin appear to be to regulate the electrical resistance across the barrier and decrease paracellular permeability. Zonula occludens proteins (ZO-1, ZO-2, and ZO-3) serve as recognition proteins for tight junction placement and connect transmembrane proteins to the actin cytoskeleton. Dissociation of ZO-1 has been shown to be associated with increased barrier permeability [2, 8].

It has been estimated that the tight junctions of the BBB prevents the brain from taking up 100% of the large (>1kD) molecule therapeutics comprising of genes and recombinant proteins as well as more than 98% of potential neurotherapeutics[9] comprising of small molecules proteins and peptides (500-1kD). The development of therapeutics that can cross the BBB is a formidable challenge, and an important one, considering that a large number of emerging therapeutics are based on peptides, recombinant proteins and genes, and are macromolecular in nature. Consequently, it is equally important to develop a suitable *in vitro* model of the Blood-Brain Barrier for rapid screening and evaluation of these therapeutics.

Panula et al.[10] first demonstrated that brain endothelial cells could be maintained in culture as a prototype *in vitro* BBB model. However, over time, these primary cultures of CNS endothelial cells lose many of the characteristics of the *in vivo* phenotype, suggesting that factors inherent to the *in vivo* environment are required to maintain an optimally functioning BBB. For example, it has been shown that brain endothelial cells become highly impermeable and exhibit extensive tight junction formation when cultured in the presence of astrocytes or astrocyte-conditioned medium (ACM) [11, 12]. The formation of these tight junctions in *in vitro* BBB models is often characterized by the expression levels of one or more of the tight junction proteins mentioned above. In addition to biochemical assays, some devices feature electrodes to measure trans-endothelial electrical resistance (TEER) across the two compartments[13, 14].

These *in vitro* cellular models have had a beneficial impact on a diverse range of scientific fields ranging from classical pharmacodynamics, pharmacokinetic and toxicological research, to drug design and discovery[15], as well as nanotechnology[16]. Traditional *in vitro* approaches use static cell-based assays in a Transwell chamber to model the BBB[17-20]. However, these static assays do not represent important morphological and physiological aspects of the microcirculatory environment in the brain and as a consequence provide little correlation or predictive ability in comparison with *in vivo* data. For instance, these models do not reproduce the BBB microenvironment comprising of endothelial cells continuously exposed to shear generated by the flow of blood across their apical surfaces.

Seeking to overcome the limitations of the static incubation approaches, researchers have developed a hollow fiber apparatus[21-23]. In this device, brain endothelial cells are cultured in the lumen of hollow fibers (mimicking capillaries vessels) and exposed to flow while astrocytes are seeded in the extra-luminal compartment to form the model BBB. The results obtained from the device for TEER and biochemical assays are very encouraging. However, the dimensions of the device are not representative of the microvasculature. Secondly, high

NIH-PA Author Manuscript

NIH-PA Author Manuscript

NIH-PA Author Manuscript

flow rates and large volumes (~ml) are needed to maintain physiological shear in the system. Finally, real-time visualization is a significant challenge with hollow fiber based systems.

A recent review[24] provided a chronological history of *in vitro* BBB models, including both static and dynamic models, but overlooked the rising field of microfluidics based cell culture models[25]. Endothelial cells have been cultured in flow based devices for over a decade for studying vascular biology[26]. These flow based devices ranged from larger parallel plate flow chambers to microfluidic based *in vivo* mimetic flow chambers. Endothelial cells of different origin can be readily cultured and monitored real-time for functional assays [27]. Taking advantage of these microfabrication technologies, a microfluidic BBB model was recently demonstrated[28] using a co-culture of endothelial cells and astrocytes cultured on a membrane filter. However, this model featured a top-bottom architecture, which limits the ability to simultaneously visualize in real-time both the vascular and neuronal sides of the BBB.

To overcome these limitations, we report on the development of a microfluidics based Synthetic Microvasculature model of the Blood-Brain Barrier (SyM-BBB). The SyM-BBB model comprises of microchannels partitioned into two side-by-side chamber by utilizing pillars or posts which mimic the use of 0.3-10μm membranes in conventional models such as the Transwell chambers. The posts in the current studies are separated by 3 μm gaps (similar to Transwell membranes used for permeation and cell migration studies), which ensures communication between the two chambers. This approach is more manufacture-friendly than other microfluidic approaches to the creation of two chamber assays, which typically use a filter or micromachined insert between top and bottom chambers. An immortalized rat brain endothelial cell line; RBE4[29, 30] is cultured in the apical chamber under fluidic shear conditions and in continuous contact with astrocyte-conditioned medium (ACM) in the basolateral chamber. RBE4 cells preserve the endothelial phenotype, show differentiation characteristics of brain endothelium in the presence of glial factors express P-glycoprotein [29, 31] and have been used for wide range of *in vitro* assays to characterize endothelial function and transport [32-34]. The basolateral chamber can house neuronal components, such as astrocytes leading to a more accurate structural representation of the BBB.

The benefits of the SyM-BBB include: (1) Realistic microcirculatory dimensions and environment, (2) physiological fluid flow and shear stress, (3) oxygen-permeable substrate allows long-term in situ cell culture and (4) real-time optical monitoring. The primary purpose of the SyM-BBB platform is to enable predictive screening, evaluation and optimization of the ability of a drug candidate to permeate the BBB. However, the device can also be used to provide an understanding of the extent of BBB dysfunction during the pathogenesis of various neurological diseases. Use of this platform, along with complementary *in silico* approaches, could accelerate the development of CNS therapeutics.

MATERIALS AND METHODS

Design of SyM-BBB Device

A common feature of the microvasculature is the presence of diverging and converging bifurcations and junctions. Hence, in order to mimic this commonly observed feature we designed the device to represent an idealized construct of the microvasculature comprising of a diverging and converging bifurcations as shown conceptually in Figure 1. The device comprises of a 200 μm wide outer chamber (apical side) separated by a central chamber (basolateral side) utilizing microfabricated gaps of 50 μm length, 3 μm width and 3 μm height. All the chambers are 100 μm deep, typical of microvascular networks observed *in vivo*. Each of these chambers is designed to have their own inlet and outlet ports for

NIH-PA Author Manuscript

NIH-PA Author Manuscript

NIH-PA Author Manuscript

individually perfusion and sampling of the media (Figure 1a). A key design feature is the use of two-layer fabrication to develop the desired 3 μm gaps between the two chambers. The 3 μm gap size was chosen to mimic the 3 μm pore size commonly used in the filters used in the Transwell apparatus for permeation and migration studies. The side view image in Figure 1b highlights the 3 μm gap, which is formed when the microfabricated device is bonded to the glass slide for creation of the final device.

Fabrication of Masters of SyM-BBB Device

Deep reactive ion etching (DRIE) was used to machine the pattern into bulk silicon substrate which allows tightly controlled etch depths [35] to yield the 3 μm gaps (Layer 1 – fine lines in Figure 2a). Subsequently, the apical and the basolateral sides (Layer 2 shown in Figure 2b) were constructed with DRIE at a constant depth of 100 μm. The masters for fabricating the SyM-BBB were developed using the following procedure. Silicon substrate was cleaned with Piranha solution and dehydrated at 200°C for 5 min. Hexamethyldisilazane (HMDS) was spin-coated at 4,000 rpm for 30 s and baked for 1 min at 95°C to functionalize the substrate with hydroxyl groups for photoresist adhesion. Shipley high resolution series S1818 photodefinable polymer was then spin-coated on the substrate at 2500 rpm for 30 s for a thickness of 1–3 μm and baked at 95°C for 1 min, followed by UV exposure with 365 nm light at ~56 mJ/cm^2 for approximately 7 s. The resist was developed in MF-319 solution to wash away the exposed resist to form the stencil (resist mask) for use with etching. Finally, Bosch Inductive Coupled Plasma (ICP) based high aspect ratio/straight sidewall capable etch process with CF3 passivation for sidewall control and SF6-O2 for etching were used in alternating cycles for making the master for the device.

SEM Imaging

SEM images of the masters were acquired using a Hitachi S-2600N (Hitachi High Technologies America, Inc., Pleasanton, CA) scanning electron microscope. Samples were coated with 50 nm of Au using a Hummer 6.2 sputtering system (Anatech Ltd., Union City, CA). An acceleration voltage of 15 kV was used for subsequent imaging. Figure 2c-f show scanning electron microscopy (SEM) images of the fabricated masters.

SyM-BBB Fabrication

Sylgard 184 Polydimethylsiloxane (PDMS) was prepared according to manufacturer's (Dow Corning, Midland, MI) instructions using standard lithography process [36]. Briefly, Sylgard 184 PDMS mixed in a ratio of 10:1 (polymer and curing agent) was poured over the developed masters in a 150 mm Petri dish, and degassed for 15 min. The polymer was then allowed to cure overnight in an oven at 65°C. Through holes, defining the inlets and outlets, were punched using a 1.5 mm punch. The bonding surfaces of the PDMS and 1″×3″ glass slide were plasma treated (200 mTorr, 18 W, 30 s) in a plasma generator (Harrick Scientific, Ithaca, NY). A seal between the PDMS and glass was achieved by heating the assembly at 75°C for 10 min on a hotplate yielding the complete device (Figure 3a). Tygon Microbore tubing with an outside diameter of 0.03″ and inner diameter of 0.01″ connected to 25-gauge stainless steel needle served as the connecting port to reagents. The entire device was autoclaved at 121°C for sterilization and stored under sterile environment until cell culture use.

Testing of SyM-BBB

Fluorescent dye, fluorescein isothiocyanate (FITC) at a concentration of 100 μg/ml was injected into both the apical and basolateral sides of the chamber to evaluate the integrity of the fabricated 3 μm gaps. As shown in 3b, the apical side and the basolateral sides are

NIH-PA Author Manuscript

NIH-PA Author Manuscript

NIH-PA Author Manuscript

fluorescent with a dark bridge between them and FITC perfused 3 μm gaps indicating an intact barrier with gaps fluidically connecting the two chambers.

Culture of RBE4 Cells in SyM-BBB Device

RBE4 cells were cultured in Eagle's Minimum Essential Medium (EMEM) and Ham's F-10 media (1:1) supplemented with 10% FBS, 1% Pen/Strep, 2 mM L-glutamine and G418 (300 μg/ml). Cells were incubated at 37°C, 95% humidity and 5% CO2 until confluent. Fibronectin (100 μg/ml) was injected into the apical side of the SyM-BBB and allowed to incubate at room temperature for 2 hours. Following this, serum free media was injected into the chamber and incubated at 37°C for 30 min for the chamber to get equilibrated with the media contents. RBE4 cells were harvested and resuspended to a final concentration of 5×10^6/ml for injection into the apical side of the basal chamber and allowed to attach for 2 hours. At the end of the 2 hours, cell media was perfused continuously on the apical side to culture the endothelial cells under fluidic shear (0.1 μl/min) for 24-48 hours.

Collection of ACM was accomplished by removal of media from confluent rat primary astrocyte cultures isolated from the cortex of newborn Sprague-Dawley rats (approximately 3 weeks post-isolation) according to our previously published methods [32, 33]. All animal protocols were approved by the Vanderbilt University Medical Center Institutional Animal Care and Use Committee (IACUC) and strictly adhered to in order to minimize pain. All animal procedures followed NIH laboratory animal care and use guidelines. The medium from the astrocytes (EMEM containing 10% heat-inactivated horse serum, 100 U/ml penicillin, 100 g/ml streptomycin, and 0.25 g/ml Fungizone (all from Invitrogen, Carlsbad, CA) was mixed with an equal volume of fresh RBE4 medium. In order to create the tight junctions, ACM mixed 1:1 with RBE4 media was injected into basolateral chamber for 48 hours to facilitate the formation of tight junctions[37]. Calcein AM (fluorescent indicator for viable and healthy cells) was injected into the apical chamber in combination with Ethidium Homodimer-1 (fluorescent indicator for membrane compromised cells) to visualize the active metabolizing cells.

SyM-BBB Characterization

The cultured RBE4 cells were subjected to optical and biochemical measurements for quantifying the tight junction formation using permeation studies, protein analysis and efflux transporter assays. Permeation studies were conducted using FITC-dextran while protein studies were conducted using Western blots. Experiments were carried out using Transwell chambers for comparison. Finally, efflux transporter assays were conducted using Rhodamine 123 and Verapamil, an L-type calcium channel blocker of the phenylalkylamine class.

FITC-Dextran Permeation Studies

Confluent layer of cells in SyM-BBB (with and without ACM) were perfused with FITC-dextran (3000–5000 Da, Sigma Aldridge, St. Louis, MO) at a concentration of 0.5 mg/ml on the apical side at a flow rate of 0.1 μl/min. At regular time points, the entire device was scanned using an automated stage (LEP, Ltd, Hawthorne, NY) and imaged using a cooled charge-coupled device (CCD) camera (Roper Coolsnap HQ2, Photometrics, Tucson, AZ) to quantify the FITC-dextran permeation in the basolateral side. The images were post-processed using NIKON Elements to yield the intensity ratio between the apical chamber and the basolateral chamber.

For the Transwell experiments, RBE4 cells were plated on a 3.0 μm polyester membrane insert (same size as the gaps in SyM-BBB). The cells were subsequently maintained in ACM and RBE4 media for 48 hours similar to SyM-BBB. At the end of 48 hours, 150 μl of

NIH-PA Author Manuscript

NIH-PA Author Manuscript

NIH-PA Author Manuscript

fresh media with FITC-dextran was added to the cells and 600 μl of media was added to the bottom chamber. At regular intervals starting at 1 minute, 100 μl of the volume was withdrawn from the bottom chamber to assess the fluorescent intensity. The withdrawn volume was replenished with fresh media to eliminate any volume dependent permeation. Experiments were repeated for RBE4 with no ACM and with no cells in the device. The intensity profiles of RBE4 (no ACM) and RBE4 (with ACM) were normalized with the intensity profiles of the cell free conditions to determine temporal evolution of FITC-dextran permeation.

Biochemical Measurements

RBE4 cells were cultured in SyM-BBB in the presence and absence of ACM as mentioned before. As a control, RBE4 were also cultured in Transwell chambers both in presence and absence of ACM. Cells were harvested in trypsin and washed with phosphate-buffered saline (PBS), ice cold RIPA (Radio Immuno Precipitation Assay) buffer (150 mM sodium chloride, 1.0% NP-40, 0.5% sodium deoxycholate, 0.1% SDS, 50 mM Tris, pH 8.0) and an additional mixture of protease inhibitors were added to cells and sonicated. Protein concentration of cell homogenates was determined with bicinchoninic acid (BCA™, Pierce, Rockford, IL) protein assay. Samples were loaded onto 10% sodium dodecyl sulfate (SDS)-polyacrylamide gels, and the separated proteins were transferred to a polyvinylidene fluoride (PVDF) membrane. Subsequently, the membranes were incubated for 1 hour with blocking solution (5% fat free dry milk in PBS) followed by incubation over night at 4°C with primary antibody for tight junction molecules (zonula occludens-1 (ZO-1) and claudin-1) and efflux transporter system; P-glycoprotein (P-gp). Following a 3X wash, the membranes were further incubated with secondary antibody for 2 hours at room temperature. Final detection was performed with enhanced chemiluminescence methodology (SuperSignal West Dura Extended Duration Substrate; Pierce, Rockford, IL) with the intensity of the chemiluminescence signal normalized with β-actin expression.

Efflux Activity of P-Glycoprotein

Efflux activity of Rhodamine 123 in RBE4 cells cultured in the presence and absence of ACM in SyM-BBB was investigated. In order to demonstrate drug inhibition studies, we also used Verapamil, an L-type calcium channel blocker of the phenylalkylamine class and a potent inhibitor of P-gp. Cells in SyM-BBB were equilibrated with 150 ng/ml of Rhodamine123 (Sigma Aldridge, St. Louis, MO) for 20 min at 37°C. After washing the cells with PBS containing 0.1% Bovine Serum Albumin (BSA), the cells were imaged for Rhodamine permeation. Subsequently, the dye was allowed to efflux for two hours at 37°C to calculate the efflux rates. RBE4 cells pre-incubated with verapamil (5 μM) for 30 min before the efflux served as a model for P-gp inhibition.

Statistical Analysis

All the experiments were run at least in triplicates with all error bars representing standard deviations. Analysis of variance (ANOVA) was used to determine significant differences between the test conditions. All values of $p<0.05$ were considered statistically significant.

RESULTS AND DISCUSSION

A confluent culture of RBE4 was formed within 24-48 hours post cell seeding in the SyM-BBB. In presence of ACM, RBE4 cells were successfully maintained at a flow rate of 0.1 μl/min until the completion of experiments (96 hours). Figure 3c and Figure 3e shows phase contrast images of confluent culture of RBE4 cells in SyM-BBB and Figure 3d and Figure 3f shows highly active cultures as indicated from the uniform concentration of calcein AM and minimal (less than 1%) presence of ethidium homodimer-1 stained endothelial cells.

NIH-PA Author Manuscript

NIH-PA Author Manuscript

NIH-PA Author Manuscript

Figure 4 shows the intensity profiles of SyM-BBB following FITC-dextran perfusion. The optically clear compartments in SyM-BBB allow real-time monitoring of the permeation of FITC-dextran, which is not possible with Transwell chambers. The top panel shows the intensity profiles at regular time points, indicating that by 60 min, the basolateral chamber of the cell-free SyM-BBB was completely perfused with FITC-dextran. However, in the case of SyM-BBB with cells but no ACM and SyM-BBB with cells and ACM, there was a significant difference in the FITC-permeation, even at 30 min. The presence of cells, even in the absence of ACM, significantly decreases the permeability of the barrier as reflected by lower FITC-dextran intensity levels in the basolateral chamber. The barrier permeability is further reduced by the use of the ACM. The decrease in FITC-dextran permeation can be attributed to the presence of cell layer and the formation of tight junctions in the presence of ACM, which block the 3 μm pores thereby reducing the diffusion of the molecules from the apical chamber to the basolateral chamber.

In order to quantitate the FITC-dextran intensity levels, we plotted the FITC-dextran permeation data, where the intensity profiles of RBE4 (no ACM) and RBE4 (with ACM) were normalized with the intensity profiles of the cell free conditions (Figure 5). The initial differences between the ACM vs. no ACM conditions vanishes rapidly in the Transwell chambers reaching no statistical significance within <30 min. However, the SyM-BBB device exhibits significantly lower permeation levels even after 60 min suggesting tight junction formation between the endothelial cells. This is particularly true for cells in the presence of ACM suggesting that the presence of ACM and flow have an additive effect, which cannot be attained under static conditions.

Expression levels of the tight junction proteins (ZO-1 and claudin-1) and the efflux transporter system (P-gp) are shown in Figure 6. Each individual data series is plotted normalized to the static Transwell experiments protein levels in the absence of ACM. The upregulation was found to be maximal for ZO-1 ($P < 0.01$), but other molecules (Claudin-1 and P-gp) were also upregulated significantly ($P < 0.05$ and $P < 0.01$, respectively) under flow in SyM-BBB with ACM amplifying the signal significantly. This is again likely due to the additive effect of flow with ACM, which will be prevalent under *in vivo* conditions. Since ZO-1 dissociation has been associated with increased barrier permeability[32] and claudins[2] establish the primary gate of the tight junction, the minimal FITC-dextran permeability and the upregulation of these proteins show that tight junctions are formed in SyM-BBB.

Following successful results on upregulation of P-gp, we assessed the efflux activity of Rhodamine 123 in RBE4 cells cultured in the presence and absence of ACM in SyM-BBB. Figure 7 shows images of rhodamine efflux in SyM-BBB. The presence of ACM in SyM-BBB allowed significant ($P < 0.05$) uptake and increased efflux compared with the RBE4 cells in the absence of ACM. In addition, although Verapamil reduces the efflux of Rhodamine 123, the efflux increases in the presence of ACM. This shows that P-gp is functionally active in SyM-BBB and that it efficiently regulates the efflux activity. Furthermore, these studies establish the modulation of the functional characteristics of SyM-BBB by known transport blockers.

CONCLUSIONS

We have developed a microfluidic based model of the blood-brain barrier (BBB), SyM-BBB, which mimics the physiological and functional environment, observed *in vivo*. SyM-BBB was fabricated using rapid and cost effective manufacturing process of soft-lithography. Rat brain endothelial cell line (RBE4) was successfully cultured in presence of astrocyte-conditioned media (ACM) under continuous perfusion for up to 96 hours.

NIH-PA Author Manuscript

NIH-PA Author Manuscript

NIH-PA Author Manuscript

Experiments were carried out with Transwell chambers using 3 μm porous membrane for comparison with 3 μm gap SyM-BBB device. In addition, real-time tracking of FITC-dextran in the SyM-BBB device was successfully demonstrated. FITC-dextran permeation studies on the endothelial cells in SyM-BBB showed tight junctions formation in contrast with Transwell chambers. Upregulation of tight junction proteins was validated by Western blot analysis of ZO-1, and claudin-1. Functional characteristics of the SyM-BBB were corroborated by upregulation of P-gp and efflux transporter studies comprising of Rhodamine 123 and its active inhibitor verapamil. SyM-BBB was able to regulate the transporting efficiencies of RBE4 cells indicating a functional representation of the *in vivo* BBB.

The developed model can have implications in drug discovery and for basic understanding of the biological signaling in the BBB physiology. Planned future work includes culture of primary endothelial cells, co-culture of endothelial cells, pericytes and astrocytes and integration of on-chip electrodes for continuous trans-endothelial electrical resistance (TEER) measurements. Other future studies could focus on the development of a medium to high throughput system for enhanced commercial viability of the SyM-BBB device.

Acknowledgments

We thank Yingchu Yu for help with cell culture and Dr. Ketan Bhatt for the illustration. We acknowledge financial support from National Institute of General Medical Sciences of the National Institutes of Health under award number R44 GM087129-02, and other NIH grants (R01 ES 07331-16; R01 ES 10563-11).

REFERENCES

1. Joó F. J Neurochem. 1992; 58:1–17. [PubMed: 1727421]
2. Abbruscato TP, Davis JP. Brain Res. 1999; 842:277–286. [PubMed: 10526124]
3. Reese TS, Karnovsky MJ. J. Cell. Biol. 1967; 34:201–217.
4. Baranczyk-Kuzma A, Audus KL, Borchardt RT. J. Neurochem. 1986; 46:1956–1960. [PubMed: 2871135]
5. Audus KL, Borchardt RT. I>Ann. N.Y. Acad. Sci. 1987; 507:9–18.
6. Iadecola C. Nat Rev Neurosci. 2004; 5:347–360. [PubMed: 15100718]
7. Hawkins BT, Davis TP. Pharmacol Rev. 2005; 57:173–85. [PubMed: 15914466]
8. Kago T T, Takagi N N, Date I, Takenaga Y, Takagi K K, Takeo S. Biochem Biophys Res Commun. 2006; 339:1197–203. [PubMed: 16338221]
9. Pardridge WM. NeuroRx. 2005; 2:3–14. [PubMed: 15717053]
10. Panula P, Joo F, Rechardt L. Experientia. 1978; 34:95–97. [PubMed: 620753]
11. Janzer JC, Raff MC. Nature. 1987; 325:253–257. [PubMed: 3543687]
12. Rubin LL, Hall DE, Porter S, Barbu K, Cannon C, Horner HC, Janatpour M, Liaw CW, Manning K, Morales J, Tanner LI, Tomaselli KJ, Bard F. J. Cell Biol. 1991; 115:1725–1735. [PubMed: 1661734]
13. Matthes F, Wölte P, Böckenhoff A, Hüwel S, Schulz M, Hyden P, Fogh J, Gieselmann V, Galla HJ, Matzner U. J Biol Chem. 2011; 286:17487–94. [PubMed: 21454621]
14. Biegel D, Spence DD, Pachter JS. Brain Res. 1995; 692:183–9. [PubMed: 8548302]
15. Mizuno N, Niwa T, Yotsumoto Y, Sugiyama Y. Pharmacol. Rev. 2003; 55:425–461. [PubMed: 12869659]
16. Lockman PR, Oyewumi MO, Koziara JM, Roder KE, Mumper RJ, Allen DD. J. Control Release. 2003; 12:271–282. [PubMed: 14644577]
17. Biegel D, Pachter JS. In Vitro Cell Dev Biol Anim. 1994; 30:581–8. [PubMed: 7820308]
18. de Vries HE, Blom-Roosemalen MC, de Boer AG, van Berkel TJ, Breimer DD, Kuiper J. Pharmacol Exp Ther. 1996; 277:1418–23.

NIH-PA Author Manuscript

NIH-PA Author Manuscript

NIH-PA Author Manuscript

19. Fitsanakis VA, Piccola G, Aschner JL, Aschner M. J Neurosci Res. 2005; 81:235–243. [PubMed: 15948148]
20. Vu K, Weksler B, Romero I, Couraud PO, Gelli A. Eukaryot Cell. 2009; 8:1803–7. [PubMed: 19767445]
21. Cucullo L, McAllister MS, Kight K, Krizanac-Bengez L, Marroni M, Mayberg MR, Stanness KA, Janigro D. Brain Research. 2002; 951:243–254. [PubMed: 12270503]
22. Cucullo L. L, Aumayr B, Rapp E, Janigro D. Curr. Op. Drug Disc. & Dev. 2005; 8:89–99.
23. Santaguida S S, Janigro D, Hossain M, Oby E, Rapp E, Cucullo L. Brain Res. 2006; 1109:1–13. [PubMed: 16857178]
24. Ribeiro MM, Castanho MA, Serrano I. Mini Rev Med Chem. 2010; 10:262–70. [PubMed: 20408804]
25. Zhang C, van Noort D. Top Curr Chem. 2011; 304:295–321. [PubMed: 21598103]
26. Van der Meer AD, Poot AA, Duits MH, Feijen J, Vermes I. J Biomed Biotechnol. 2009:823148. [PubMed: 19911076]
27. Prabhakarpandian B, Shen MC MC, Pant K, Kiani MF. Microvasc Res. 2011; 82:210–220. [PubMed: 21763328]
28. Booth R, Kim H. Lab Chip. 2012; 12:1784–92. [PubMed: 22422217]
29. Roux F, Durieu-Trautmann O, Chaverot N, Claire M, Mailly P, Bourre JM, Strosberg AD, Couraud PO. J. Cell. Physiol. 1994; 159:101–113. [PubMed: 7908023]
30. Durieu-Trautmann O, Federici C, Creminon C, Foignant-Chaverot N, Roux F, Claire M, Strosberg AD, Couraud OP, P O. J. Cell. Physiol. 1993; 155:104–111. [PubMed: 7682220]
31. Begley DJ, Lechardeur D, Chen ZD, Rollinson C, Bardoul M, Roux F, Scheman D, Abbott NJ. J. Neurochem. 1996; 67:988–995. [PubMed: 8752104]
32. Yang J, Mutkus LA, Strandhoy JW, Sumner D, Stevens JT, Eldridge JC, Aschner M. Mol Brain Res. 2001; 97:43–50. [PubMed: 11744161]
33. Yang J, Aschner M. Neurotoxicology. 2003; 24:741–5. [PubMed: 12900088]
34. Dallas S, Zhu X, Baruchel S, Schlichter L, Bendayan R. J. Pharmacol. Exp. Ther. 2003; 307:282–290. [PubMed: 12893836]
35. Chen SC, Lin YC, Wu JC, Horng L, Cheng CH. Microsystems Technologies. 2007; 13:465–474.
36. Prabhakarpandian B, Pant K, Scott RC, Patillo CB, Irimia D, Kiani MF, Sundaram S. Biomed Microdevices. 2008; 10:585–95. [PubMed: 18327641]
37. Aschner M M, Sonnewald U, Tan KH. Brain Pathol. 2002; 12:475–81. [PubMed: 12408234]

NIH-PA Author Manuscript

NIH-PA Author Manuscript

NIH-PA Author Manuscript

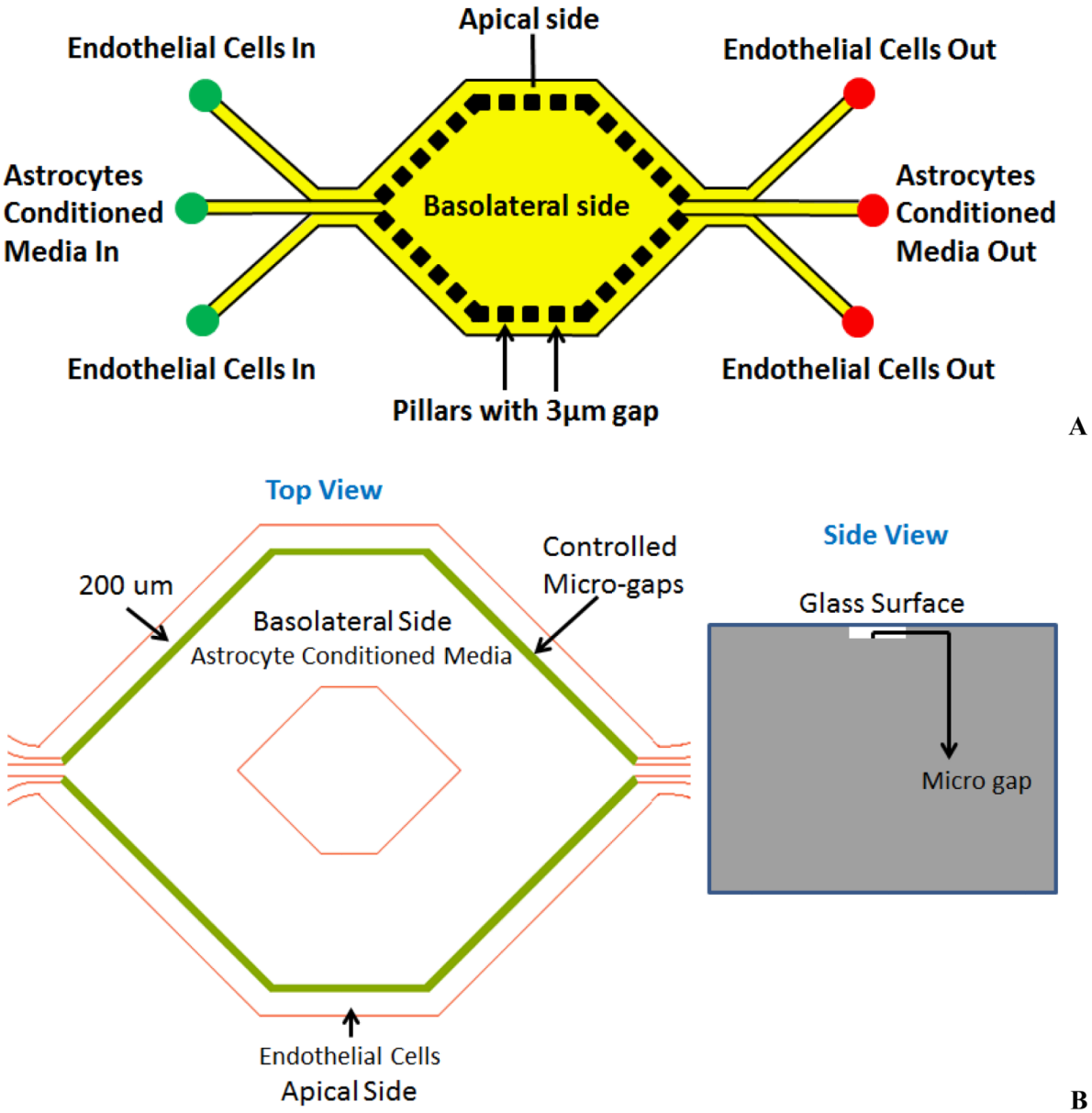

Figure 1.

SyM-BBB Model.

(A). Concept showing the apical and basolateral side separated by 3 μm gaps formed by microfabricated pillars. Apical side contains endothelial cells while basolateral side contains astrocytes conditioned media. The design is based on the idealized concept of the microvasculature comprising of diverging and converging bifurcations. (B). Schematic showing the top view and the side view highlighting the 3 μm gap formed between the glass surface and the polymer. The basolateral chamber is supported in the center by a support structure to prevent collapse of the top of the microfabricated chamber.

NIH-PA Author Manuscript
NIH-PA Author Manuscript
NIH-PA Author Manuscript

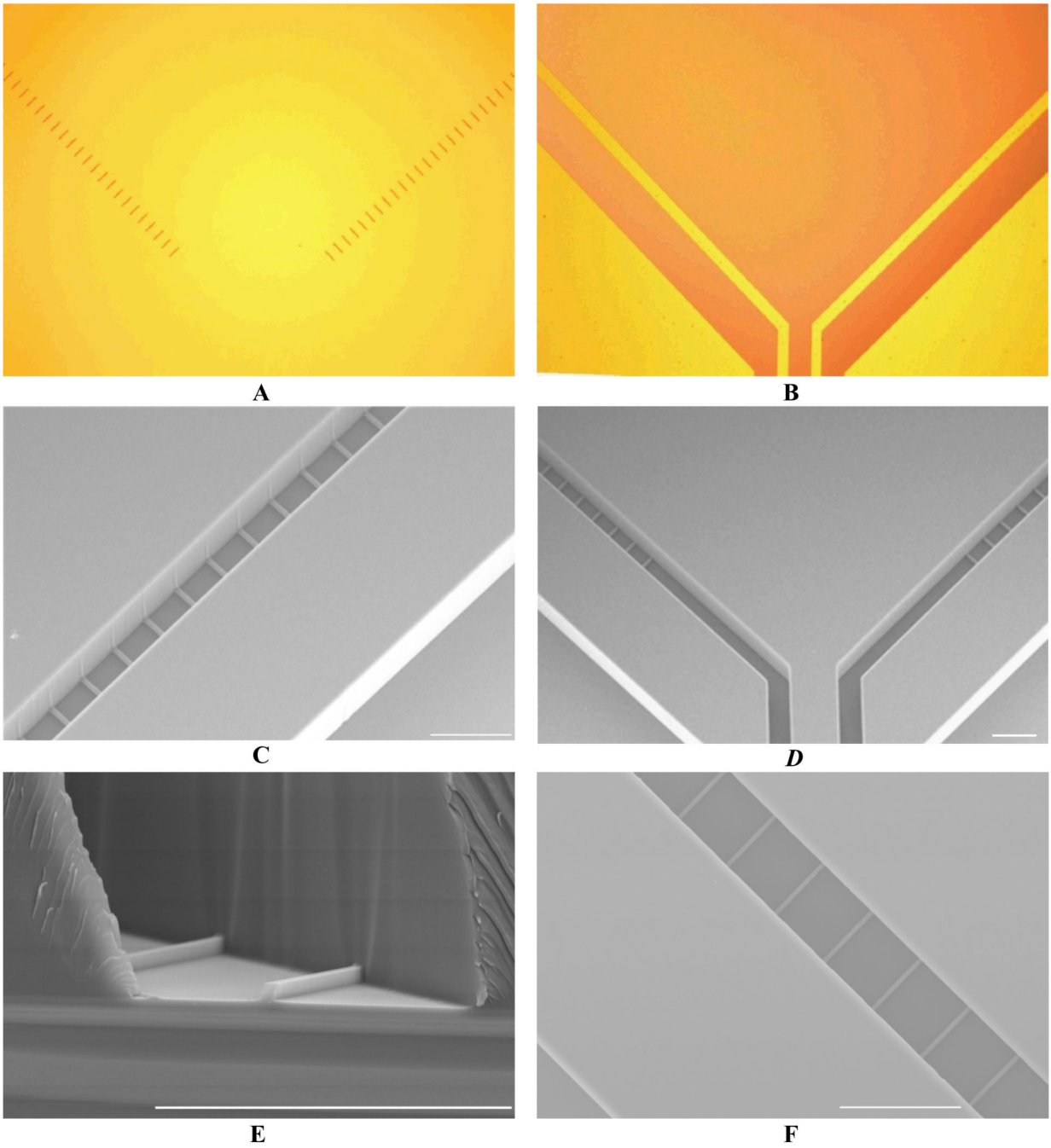

Figure 2.

SyM-BBB Fabrication.

(A-B) Photomask for creating the 3 μm gaps and fluidic channels representing the apical and basolateral chambers. (C-D) SEM of the 3 μm gaps and apical and basolateral fluidic channels. (E-F) Side view and top view SEM of the 3 μm gaps. Scale bars are 100 μm

NIH-PA Author Manuscript

NIH-PA Author Manuscript

NIH-PA Author Manuscript

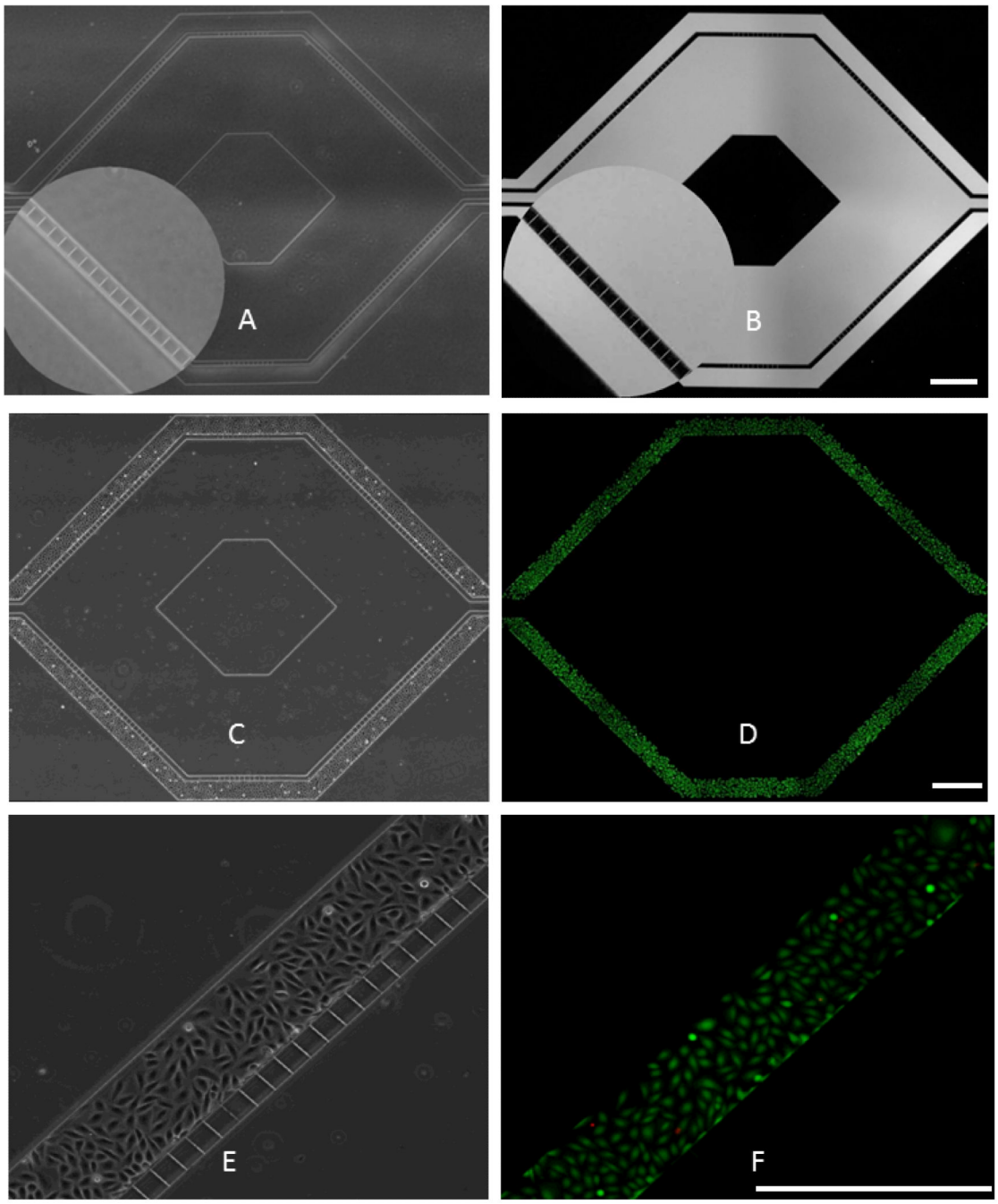

Figure 3.

(A) Fabricated SyM-BBB with 3 μm gaps. (B) FITC dye perfused SyM-BBB. Circle shows magnified image highlighting intact gaps with fluorescent dye. (C) Confluent culture of endothelial cells in SyM-BBB. (D) Highly viable cells are indicated by intense green stain (Calcein AM) and minimal red stain (Ethidium Homodimer-1). (E-F) Magnified image of endothelial cells in phase contrast and fluorescence. Scale bars are 500μm.

NIH-PA Author Manuscript

NIH-PA Author Manuscript

NIH-PA Author Manuscript

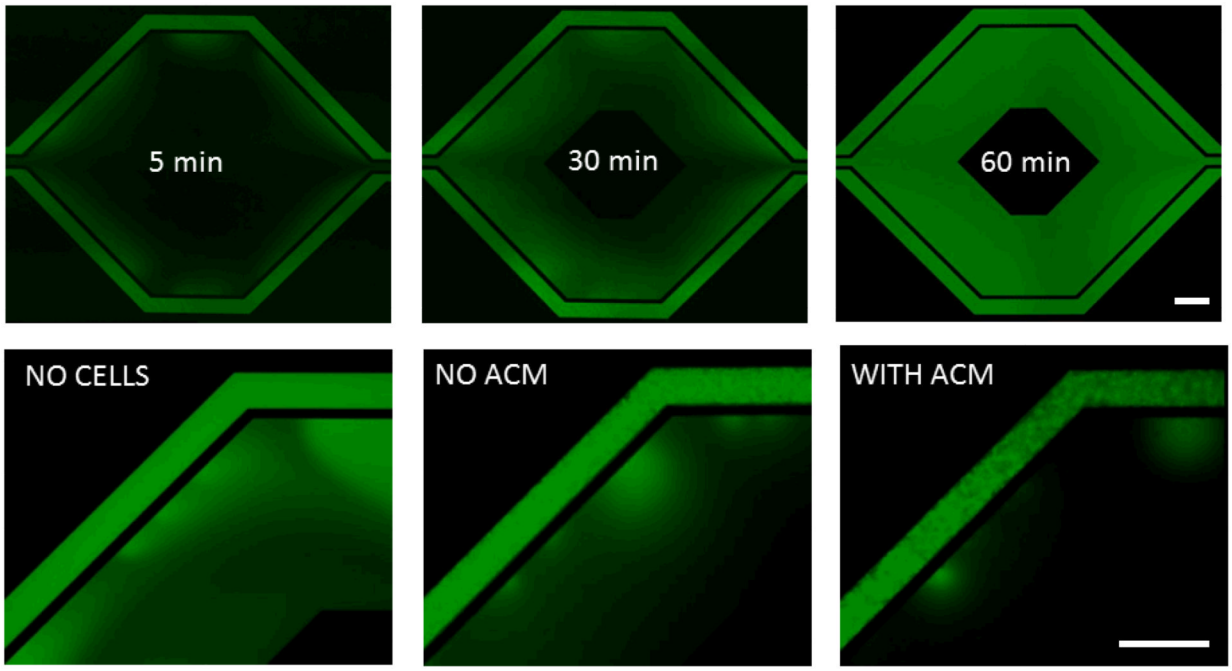

Figure 4.

FITC-Dextran permeation in SyM-BB from the apical side to the basolateral side.

Top Panel: Time-lapse FITC-dextran permeation in cell free SyM-BBB.

Bottom Panel: Magnified view showing comparison between test conditions in SyM-BBB. “No cells” indicates SyM-BBB without any endothelial cells. “No ACM” indicates SyM-BBB with endothelial cells in absence of ACM and “With ACM” indicates SyM-BBB with endothelial cells in presence of ACM. SyM-BBB with endothelial cells but without ACM shows significantly less permeation compared to cell free SyM-BB. SyM-BBB in presence of ACM shows minimal perfusion compared to the no cell and no ACM test conditions. All images are at 30 minutes post injection of FITC-Dextran. Scale bars are 500μm.

NIH-PA Author Manuscript

NIH-PA Author Manuscript

NIH-PA Author Manuscript

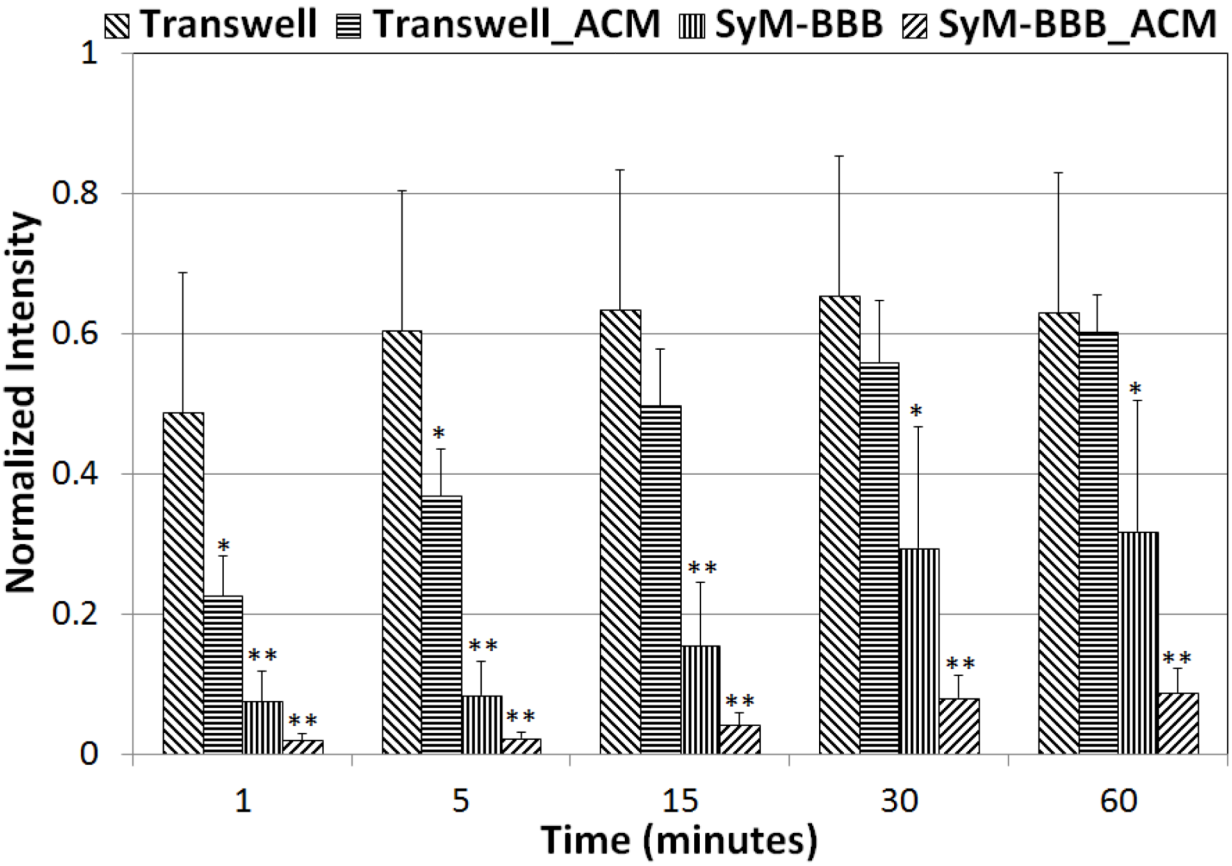

Figure 5.

FITC-dextran permeation in Transwell chamber and SyM-BBB. Data is normalized with the intensity of the intial concentration of FITC-dextran. For Transwell chambers, the initial differences between the ACM vs. no ACM conditions shows no statistical significance by 15 min. In contrast, SyM-BBB device shows significant difference even after 60 min of FITC-dextran injection, suggesting that SyM-BBB can be used to study drug permeation. All data values are mean with error bars representing standard deviation. $p < 0.05$ (*), $p < 0.01$ (**).

NIH-PA Author Manuscript

NIH-PA Author Manuscript

NIH-PA Author Manuscript

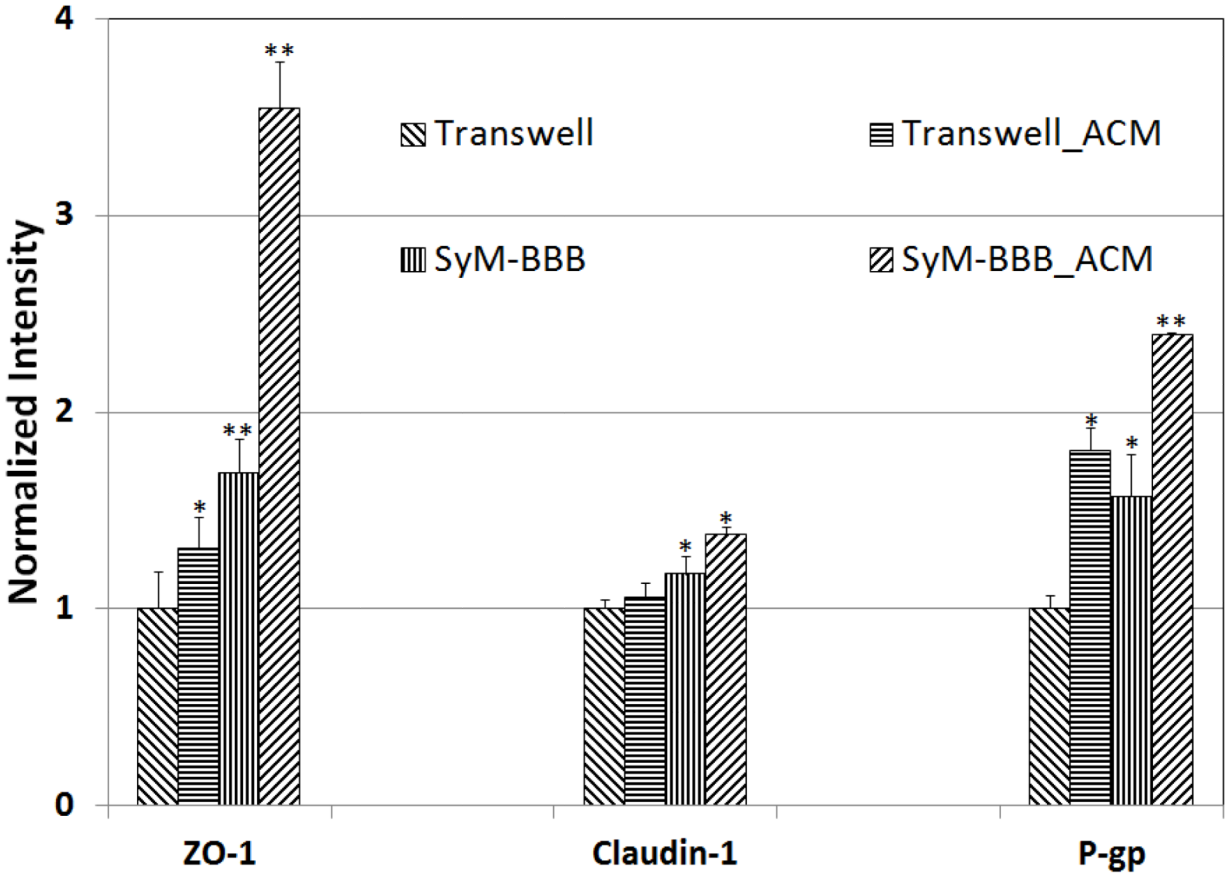

Figure 6.

Western blot analysis of tight junction molecules: zonula occludens-1 (ZO-1) and claudin-1) and efflux transporter system: P-glycoprotein (P-gp) in Transwell chamber and SyM-BBB. ZO-1 levels are upregulated significantly in SyM-BBB_ACM compared to Transwell with or without ACM and SyM-BBB with no ACM. In addition, SyM-BBB without ACM also shows significant upregulation of ZO-1 compared to Transwell. Claudin-1 levels although significantly upregulated compared to Transwell are of lower intensity compared to ZO-1. P-gp levels are also significantly upregulated. $p<0.05$ (*), $p<0.01$ (**)

NIH-PA Author Manuscript

NIH-PA Author Manuscript

NIH-PA Author Manuscript

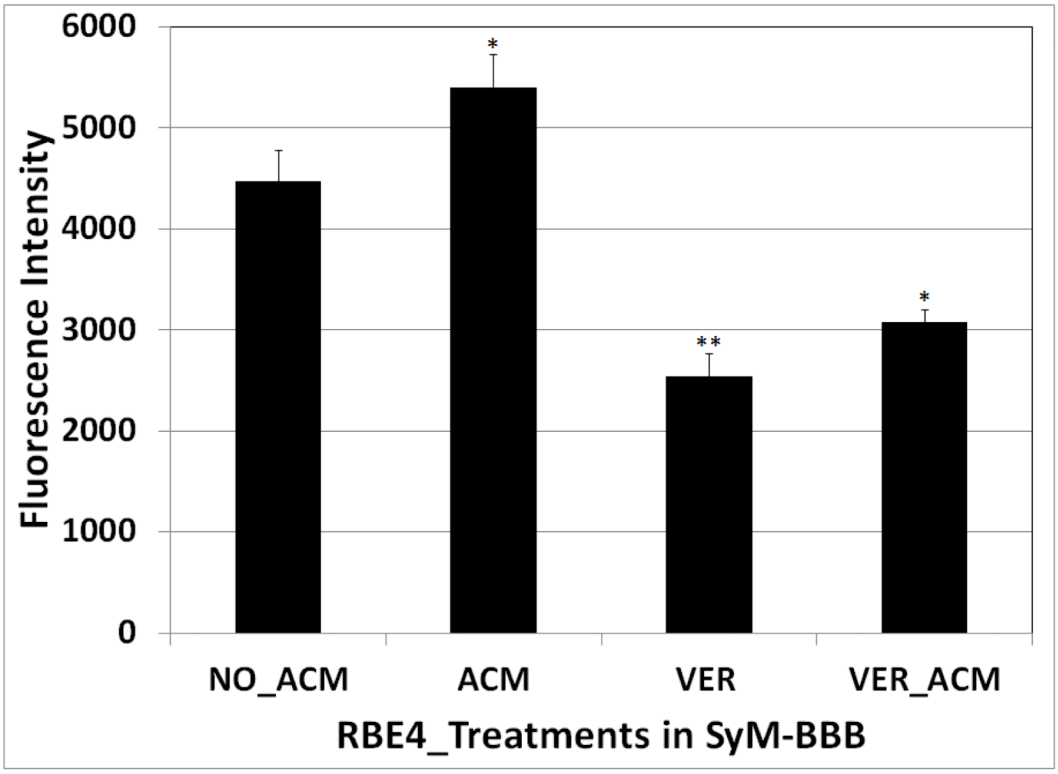

Figure 7.

Rhodamine123 efflux in SyM-BBB. RBE4 cells were assayed for efflux activity using fluorescently labeled Rhodamine 123. Verapamil (inhibitor of P-gp) was used to determine the functionality of the BBB under inhibitory conditions. “No_ACM” indicates SyM-BBB with endothelial cells in absence of ACM and “ACM” indicates SyM-BBB with endothelial cells in presence of astrocyte conditioned medium, “VER”indicates SyM-BBB in presence of verapamil and “VER_ACM” indicates SyM-BBB in presence of verapamil and ACM. ACM perfused cells exhibit signfiicantly higher efflux of Rhodamine 123 indicating functional P-gp activity. Reduction in presence of Verapamil indicates inhibition of P-gp activity while efflux activity increase in presence of ACM compared to verpamil again indicates reversal of P-gp activity demonstrating a fully functional and modulating BBB. $p < 0.05$ (*), $p < 0.01$ (**)